JOURNAL OF CATALYSIS **61**, 170–183 (1980)

Studies of the Hydrogen Held by Solids

XXV. The Proton Resonance From H_2 Adsorbed on Alumina and Molybdena–Alumina Catalysts[1]

ALEXANDER C. CIRILLO, JR., J. M. DEREPPE, AND W. KEITH HALL[2]

Department of Chemistry, University of Wisconsin, Milwaukee, Wisconsin 53201

Received May 21, 1979

An NMR study of the low-temperature adsorption of hydrogen on alumina and molybdena–alumina catalysts has led to the detection of at least two, and on extensively reduced molybdena–alumina catalysts, three, types of adsorbed hydrogen species. A single, averaged absorption line was observed originating from fast exchange between a small amount of strongly chemisorbed gas and the majority species which was molecular and much more weakly held. On alumina and unreduced molybdena–alumina the strongly chemisorbed species is also thought to be molecular, but evidence was obtained for dissociative adsorption on extensively reduced catalysts at low coverage. The signal width for the latter was that of the alumina surface hydroxyl groups; it remained constant with increasing coverage while the signal intensity increased. About 6×10^{13} H_2/cm^2 were adsorbed at the knee of the curve, where averaging with the narrow band from the weakly adsorbed gas first became detectable. Interestingly, this broad signal disappeared when the extensively reduced surface was poisoned with about 3×10^{13} O(atoms)/cm^2. NO also acted as a poison but was less selective. These studies provided a bridge between the present studies of the low-temperature adsorption of hydrogen and previous data for the hydrogenation of propylene around room temperature. Since both O_2 and NO are known to poison the catalytic hydrogenation at 21°C, it was concluded that the site responsible for the low-temperature adsorption and dissociation of H_2 may be identified with those responsible for the catalytic process. Studies of the longitudinal relaxation process over the alumina catalyst showed that T_1 decreased (at constant coverage) with increasing adsorption temperature, as expected for relaxation by translational diffusion when $\omega\tau \gg 1$. At the same time, T_1 decreased (at constant coverage) as the extent of dehydroxylation increased, suggesting an interaction with ^{27}Al (CUS). Intermolecular processes, e.g., collisions between adsorbate molecules, were not important in the relaxation mechanism as judged by the fact that T_1 remained constant when D_2 was substituted for part of the H_2 at constant pressure. The signal from reduced molybdena–alumina catalysts could not be saturated. For the alumina catalysts, at constant coverage the linewidth decreased as the adsorption temperature increased, but increased with extent of dehydroxylation. For molybdena–alumina the linewidth increased with the extent of reduction. Since only *ortho*-H_2 is detected by NMR, the kinetics of the first-order approach to equilibrium could be monitored in the adsorbed phase. Since the total adsorption was measured volumetrically, and the *ortho*-H_2 by NMR, the separation factor could be calculated in the adsorbed phase. As expected, values obtained (~2.0) indicated an enrichment of *ortho*-H_2 above the equilibrium value in the gas phase.

INTRODUCTION

Generally, heterogeneous catalysts which are effective for hydrogenation reactions also catalyze the isotopic exchange of H_2 with D_2 and the allotropic conversion of H_2. The exact nature of the "activated" hydrogen in these reactions remains uncertain, although considerable speculation on this subject already exists (*1–4*). Infrared studies (*3, 5*) have provided strong support for dissociative adsorption of hydrogen on certain oxides, but until recently the evidence for chemisorbed molecular hydrogen

---

[1] This work was begun at the Mellon Institute in 1969 (J.M.D. and W.K.H.); it was completed at University of Wisconsin–Milwaukee, in 1979 (A.C.C. and W.K.H.). The earlier work dealt exclusively with a very pure alumina catalyst.

[2] To whom all correspondence should be addressed.

0021-9517/80/010170-14$02.00/0

has been less convincing. For years the principal, nonmechanistic evidence for the latter has been the rather low isosteric heats of adsorption reported (*6*). More recently, however, the chromatographic separation of the isotopes and allotropes of hydrogen have been interpreted in terms of a molecular species (*7*, *8*), and Kokes and coworkers (*9*) have identified bands in the infrared spectra from hydrogen adsorbed on zinc oxide which were clearly due to the stretching vibrations of the perturbed H_2, HD, and D_2 molecules. Presently, existence of such species on ZnO (*9*), chromia (*4*), and molybdena–alumina (*10*) has strong support, although direct spectroscopic evidence is available only for ZnO.

For the same molybdena–alumina catalysts used in the present work, Millman and Hall (*10*) have found that the amount of irreversibly adsorbed hydrogen at 77 K increased with the extent of reduction of the catalyst. Their results also indicated molecular chemisorption at 77 K on oxidized or slightly reduced catalysts ($e/\mathrm{Mo} < 1.0$), similar to that observed for chromia (*4*). Extensive reduction ($e/\mathrm{Mo} > 1.1$), however, led to the H_2–D_2 exchange at 77 K in experiments where the catalyst acted as a chromatographic column (*4*), suggesting that the chemisorbed species was dissociating on the catalyst surface. Thus, at least three different types of adsorbed hydrogen must be dealt with in the present work, viz., (i) a dissociatively adsorbed hydrogen which formed hydroxyl groups detectable by NMR at low coverage on extensively reduced catalysts, (ii) a chemisorbed molecular species which could not be observed directly, but the effect of which was apparent in the averaged linewidth of the NMR signal, and (iii) a still more weakly chemisorbed species, which dominated the observed spectra at high coverages; the latter species exhibited most of the properties of a physically adsorbed molecule, but contributed to the chromatographic separation factor in a way suggesting site-selective molecular chemisorption. This was supported (*10*) by the fact that the adsorption isotherms were fitted by the Freundlich law and that the coverage at most amounted to only a few percent of the surface. Nevertheless, for the lack of a better term we will call this species "physisorbed." The NMR study presented herein is concerned directly with the nature of these adsorption processes.

Kazansky and co-workers (*11*, *12*) derived equations relating the broadening of NMR lines to the relative amounts of chemisorption and physisorption and applied them to the system ethylene adsorbed on silica–alumina (*12*); equilibrium constants for several temperatures were calculated and the heat of physical adsorption was determined. Insofar as possible we have applied this formalism in the treatment of our data.

EXPERIMENTAL

Catalysts

Two alumina samples were examined. One of these (GA-63) was a very pure alumina prepared by the neutral hydrolysis of aluminum isopropoxide. It was a mixture of η- and γ-alumina having a surface area of about 300 m^2/g. The total metallic impurity level measured by spark spectral analysis was less than 50 ppm. This alumina was from the same batch used in our earlier studies of hydrogen adsorbed on dehydroxylated alumina catalysts (*7*, *8*).

The other material was the support used for our molybdena–alumina catalyst. It was Ketjen CK-300 γ-alumina and had a surface area of 192 m^2/g (N_2 BET). The main impurities were Ca, Cr, Cu, Mg, and Si with less than 50 ppm total paramagnetic impurities and a total metallic impurity level of less than 100 ppm. As described earlier (*13*), the molybdena–alumina catalyst (8% Mo) was prepared by the incipient wetness technique using a solution of ammonium paramolybdate followed by drying and calcining at 550°C. The surface area of this modified alumina catalyst was 185 m^2/g (N_2 BET), and did not change upon reduction with H_2 up to 550°C.

Besides the two aluminas, a total of ten catalyst samples taken from the same batch of molybdena–alumina were used in the various studies described below. In all cases, volumetric and NMR measurements were made on the same sample to avoid the effect of slight variations in pretreatment and/or sample preparation. The reproducibility of the NMR results was tested by repeating the experiments several times. In general reproducibility was within ±5%.

Equipment and Procedures

Conventional high-vacuum systems were employed. In the work with the GA-63 alumina the *in situ* adsorption measurements were made in the NMR probe using an adjacent BET system. Since only the *ortho* molecules are detected by NMR, the data presented are for equilibrium mixtures at the experimental temperature unless otherwise specifically noted.

In all cases, catalyst samples to be investigated were pretreated and/or reduced in a separate conventional all-glass high-vacuum system using either dried flowing gases or an attached circulation loop containing a glass magnetic circulation pump. The apparatus and reduction procedures have been detailed elsewhere (*13*). A cold trap in the loop permitted the quantitative removal of H_2O generated in either the reduction or reoxidation steps; volumetric determinations of the collected H_2O could be made after removal of all other gases from the system. All gases were of CP grade and were dried and purified by conventional means before introduction into the system.

Hydrogen Adsorption

Measurements were made at indicated temperatures either *in situ* in the NMR apparatus (GA-63) or in a separate apparatus (all other catalysts) with the sample immersed in the same Dewar used in the NMR probe. For the latter, about 1 g of sample was placed in a special Pyrex recirculation reactor which was fitted with an auxiliary stopcock and ground-glass joint as well as a 10-mm-o.d. NMR tube as sidearms running perpendicular to the axis of the reactor. Following reduction or appropriate pretreatment, the sealed tube was removed from the apparatus and the evacuated sample was poured into the NMR tube which was then immersed in liquid nitrogen for any subsequent volumetric or NMR measurements. The sample was kept at 77 K during the entire series of experiments. The H_2 adsorption isotherm was determined in the usual way using the appropriate expansion factors and dead space determinations previously measured with purified He. Each point on the isotherm was taken just prior to removal of the tube (always immersed in liquid N_2 in the Dewar constructed to fit the NMR probe) and its subsequent transfer to the NMR apparatus. The level of the liquid was carefully controlled during all experiments to avoid changes in the equilibrium pressure above the sample. This factor contributed the greatest error at very low coverages where both the amount adsorbed (V_{ads}) and the NMR linewidth (ΔH_{pp}) were sensitive functions of pressure.

NMR Measurements

These were made with a Varian E-115 spectrometer equipped with a 15-in. magnet and a WL-210 variable oscillator operating in a frequency range between 3 and 35 MHz. A Northern Scientific NS-560 computer of average transients was interfaced with the spectrometer to allow for accumulation and averaging of data. All linewidths were corrected for finite modulation using the usual formulas (*14*).

RESULTS

Hydrogen Adsorption on Alumina

At low temperatures (77–120 K), at least three types of ^1H nuclei were present: those of the hydroxyl groups remaining on the surface of the oxide after pretreatment, those of the free H_2 molecules in the gas phase, and those of the adsorbed hydrogen. However, under the experimental condi-

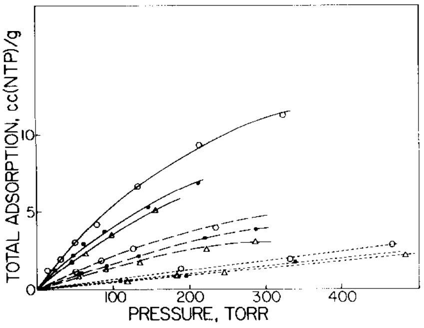

FIG. 1. Hydrogen adsorption isotherms for pure alumina (GA-63) made *in situ* in the NMR probe after vacuum pretreatment elsewhere. Pretreatment temperature (°C): ○, 550; ●, 450; △, 350. Experiment temperature (°K): ——, 80; – – –, 100; - - -, 120.

tions (77 K and hydrogen pressures less than 400 Torr) only the ^1H nuclei of the adsorbed species could be detected by NMR.

The hydrogen adsorption isotherms for the pure alumina samples (GA-63) pretreated at various temperatures are shown in Fig. 1. A systematic increase in the amount adsorbed occurred as the pretreatment temperature was raised, despite a gradual decrease in the surface area with increasing pretreatment temperature. The samples were evacuated for 4 to 8 h at the indicated temperature in the NMR tube and transferred to the probe without exposure to air. The measured surface areas were 312, 309, and 247 $m^2\ g^{-1}$ for pretreatments at 425, 500, and 600°C, respectively. These treatments dehydroxylated the surface to increasingly greater extents. The defect centers produced (anion vacancies) provided sites for the molecular chemisorption of H_2 (*7*).

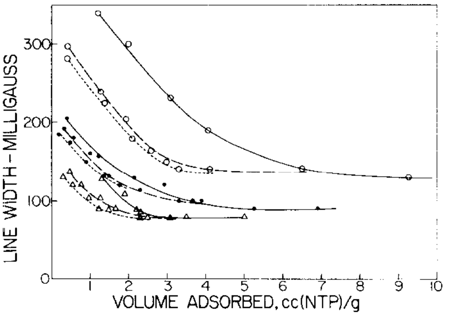

FIG. 2. A plot of observed linewidth at 15.1 MHz versus amount adsorbed for low-temperature H_2 adsorption. Pretreatment temperature (°C): ○, 550; ●, 450; △, 350. Experiment temperature (°K): ——, 80; – – –, 100; - - -, 120.

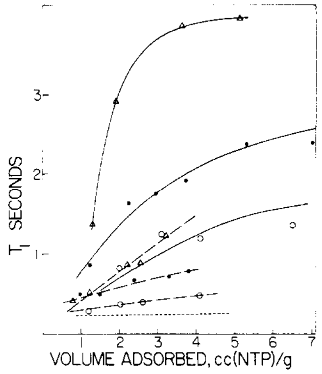

FIG. 3. A plot of the longitudinal relaxation time (T_1) versus amount adsorbed for low-temperature H_2 adsorption. The pretreatment temperatures were 550 (○), 450 (●), and 350°C (△) and the adsorption temperatures were 80 (——), 100(– – –), and 120 K (- - -), respectively.

The linewidth of the NMR signal is plotted as a function of the amount adsorbed in Fig. 2. The width increased with the extent of dehydroxylation and was greater the lower the temperature. Figure 3 shows that T_1 (saturation method) was strongly dependent upon surface coverage, especially for that fraction of H_2 molecules strongly held; T_1 decreased with increasing extent of dehydroxylation and increasing temperature. Finally, T_1 was determined for adsorbed mixtures of H_2 and D_2 on the alumina pre-

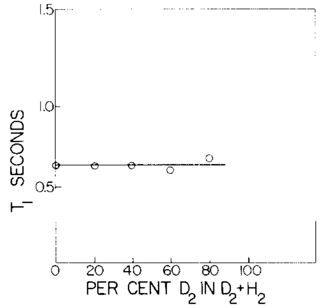

FIG. 4. A plot of (T_1) versus percentage composition for various H_2–D_2 mixtures adsorbed on pure alumina pretreated at 550°C.

treated at 550°C. The invariance of T_1 with H_2–D_2 composition at constant pressure is shown in Fig. 4. The H_2–D_2 exchange was immeasurably slow at this temperature (*10*).

Separation Factor

Since the integrated intensity of the NMR signal measures the concentration of *ortho*-hydrogen molecules (in the absence of paramagnetism) and the total adsorption was measured volumetrically, the (*ortho*–*para*) ratio in the adsorbed phase could be calculated. Since the equilibrium gas-phase concentrations are fixed by the temperature of the experiment, a separation factor may be calculated as

$$S = \frac{(o/p)\text{adsorbed phase}}{(o/p)_{\text{eq}}\ \text{gas phase}}. \quad (1)$$

Such data are reported in Table 1.

The molecular *ortho*–*para*-H_2 conversion over the same alumina catalyst has been previously studied (*8*). The NMR technique is well suited to follow this process in the adsorbed phase; as the *ortho*- to *para*-H_2 ratio changes, as the reaction proceeds, the change in signal intensity of *ortho*-H_2 may be monitored with time. All other techniques measure gas-phase values. Figure 5 is a plot of $\ln(I - I_\infty)$ versus time, i.e., the first-order relationship between the distance from equilibrium and time. These data show that all other NMR measurements for adsorbed hydrogen were made with equilibrium mixtures.

TABLE 1

The *ortho*-*para*-H_2 Separation Factor on Alumina (GA-63) at 80 K Measured by NMR

Pretreatment temp (°C)	Equilibrium pressure (Torr)	Adsorbed *ortho*-H_2[a] (molec/g × 10^{-19})	Total amount adsorbed, Volumetric (molec/g × 10^{-19})	Separation factor
350	28.4	2.56	3.14	3.53
	44.4	2.98	4.59	1.68
	65	4.75	6.75	2.23
	99.2	6.87	9.45	2.50
	156.2	9.39	13.77	2.01
450	24.8	2.2	3.51	1.57
	47.4	3.6	5.62	1.63
	60.5	5.7	7.02	4.05
	92	7.8	10.0	3.38
	145	10.2	14.3	2.32
	211.5	14.0	18.9	2.70
550	14	2.08	2.7	3.14
	30.8	4.34	5.4	3.84
	52.9	5.96	8.4	2.29
	77.8	7.75	11.61	1.88
	133.5	13.88	17.82	3.30
	2.16.5	18.69	24.8	2.86

[a] This was measured by comparison of the NMR first moment at 80 K with that of a suitable aqueous $MnCl_2$ solution at room temperature; corrections for temperature were made assuming the Curie–Longevin equation.

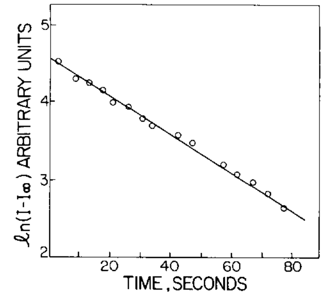

FIG. 5. A plot of ln $(I - I_\infty)$ versus time showing that the *ortho*–*para*-H_2 conversion is first order in the distance from equilibrium.

Hydrogen Adsorption on Molybdena–Alumina Catalysts

Isotherms at 77 K for H_2 on catalysts reduced to various extents are shown in Fig. 6; included in this figure is the isotherm for the pure alumina support. All samples were pretreated at 500°C and were reduced as described previously (*13*). The index *e*/Mo is a measure of the average oxidation state; it is the average number of electrons below Mo^{6+} to which the catalyst has been reduced (*15*). The total amount adsorbed increased with the extent of reduction, in agreement with the studies of Millman and Hall (*10*).

The change in linewidth with amount adsorbed for various extents of reduction is shown in Fig. 7, and both the volumetric and NMR data are summarized in Table 2. The linewidth increased with extent of reduction, particularly at low coverages. Perhaps significantly, a "plateau" appeared for

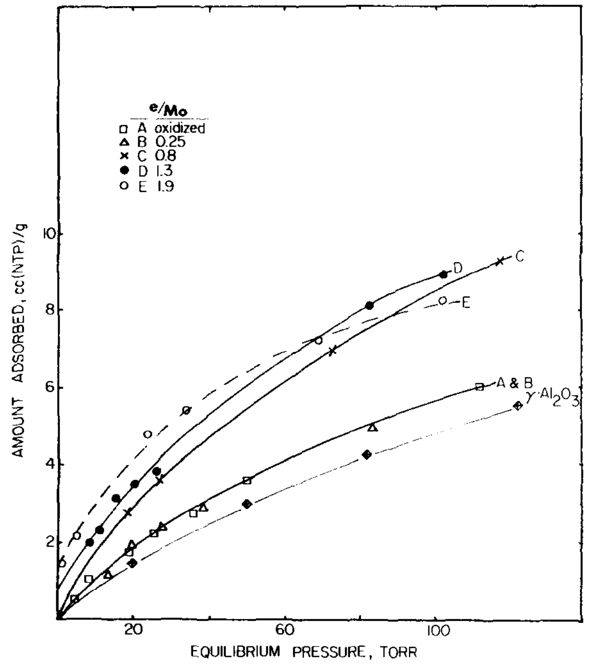

FIG. 6. Hydrogen adsorption isotherms at 77 K for molybdena–alumina catalysts at various extents of reduction. The isotherm for the pure γ-alumina support has been included.

samples with $e/\mathrm{Mo} > 1.1$. The high-pressure (high coverage) limits of linewidth are also included in Table 2 (see later). Figure 8 compares the change in linewidth with amount adsorbed observed for the oxidized catalyst with that for the pure alumina support.

Effects of Poisons

Figure 9 shows the H_2 adsorption isotherm at 77 K for a molybdena–alumina catalyst reduced to $e/\mathrm{Mo} = 1.7$ both with and without oxygen poisoning. These data were taken in successive experiments on

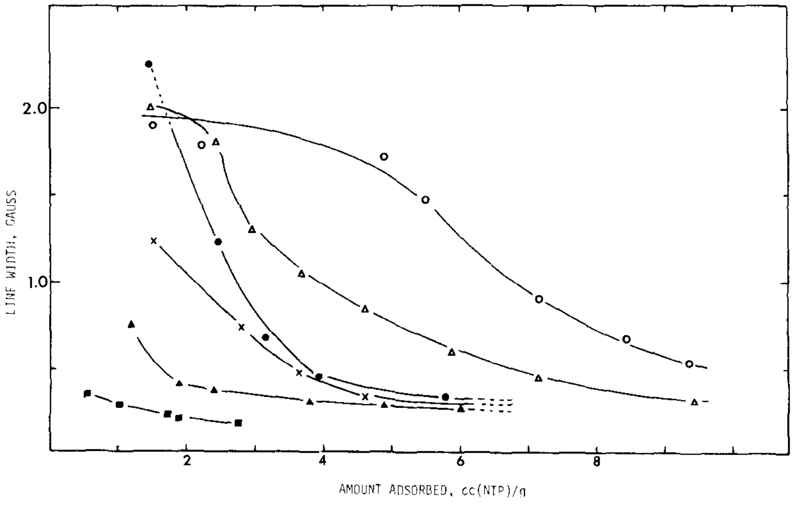

FIG. 7. A plot of observed linewidth at 35 MHz versus amount adsorbed for H_2 adsorption at 77 K on 8% Mo/Al_2O_3 reduced to $e/\mathrm{Mo} = 0.0$ (■), 0.25 (▲), 0.8 (X), 1.1 (●), 1.4 (△), and 1.7 (○).

TABLE 2

A Summary of the Volumetric and NMR Data for H_2 Adsorption at 77 K on Alumina and 8% Molybdena–Alumina Catalysts

Sample	Equilibrium pressure (Torr)	Volume adsorbed (cm^3/g)	Linewidth[a] (G)
γ-Alumina (support)	4.90	0.37	0.94
	22.40	1.63	0.25
	47.80	2.97	0.20
	83.70	4.35	0.16
	104.40	5.00	0.16
	(400)	—	0.08[b]
Molybdena–alumina oxidized	4.70	0.54	0.34
	8.80	1.02	0.28
	19.15	1.73	0.23
	19.55	1.90	0.20
	26.00	2.31	0.22
	36.40	2.76	0.17
	50.10	3.60	—
	113.15	6.00	—
	(400)	—	0.12[b]
$e/Mo = 0.25$	10.40	1.19	0.75
	19.95	1.89	0.41
	27.65	2.39	0.37
	55.30	3.79	0.30
	83.35	4.89	0.28
	121.10	6.02	0.26
	(400)	—	0.26[b]
$e/Mo = 0.75$	7.20	1.52	1.23
	18.15	2.80	0.74
	27.30	3.64	0.48
	38.75	4.60	0.33
	73.30	6.92	—
	117.60	9.44	0.30
	210.10	13.75	0.31
	(400)	—	0.26[b]
$e/Mo = 1.1$	8.40	1.47	2.25
	18.00	2.55	1.23
	24.60	3.17	0.68
	37.00	3.94	0.43
	63.05	5.79	0.33
	98.25	7.85	0.35
	(400)	—	0.33[b]
$e/Mo = 1.4$	7.40	1.46	2.0
	17.95	2.43	1.8
	25.30	2.97	1.3
	36.50	3.68	1.05
	54.60	4.62	0.85
	84.90	5.89	0.70
	148.00	7.15	0.45
	(400)	—	0.33[b]
$e/Mo = 1.7$	0.75	1.52	1.9
	5.30	2.23	1.78
	15.50	3.16	1.63
	24.20	4.90	1.72
	34.35	5.51	1.47
	69.25	7.16	0.91
	102.75	8.45	0.68
	135.15	9.37	0.54
	(400)	—	0.35[b]

[a] Corrected for finite modulation amplitude (*14*).

[b] High-pressure limit (see text).

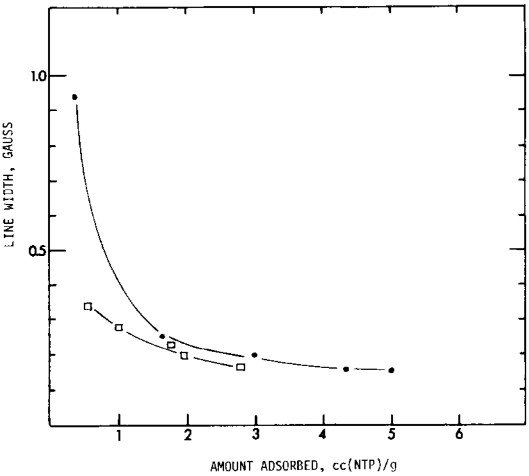

FIG. 8. A plot of the observed linewidth at 35 MHz versus amount adsorbed for H_2 adsorption at 77 K on the pure γ-alumina support (●) and on an unreduced molybdena–alumina catalyst (□).

the same catalyst. The isotherms (and NMR data) were first determined on the unpoisoned sample and then the experiments were repeated after O_2 addition. To poison the adsorption, 2.53 cm^3/g of pure O_2 was pulsed onto the reduced catalyst at 195 K. The sample was evacuated for 15 min at 195 K and subsequently quenched to 77 K for the H_2 adsorption measurements. Prior studies (*17*) indicated that this treatment results in the irreversible adsorption of 1.5 cm^3(NTP)/g of O_2 for a catalyst reduced to $e/Mo = 1.7$. The NMR data obtained concurrently with the volumetric data are shown in Fig. 10. The observed linewidths for the poisoned catalyst were comparable with those observed on a catalyst reduced to $e/Mo \sim 0.2$; they were much smaller than those originally observed. The effect was not due to reoxidation of the catalyst, since the amount of O_2 used could only change the extent of reduction from $e/Mo = 1.7$ to 1.4, providing this process occurred at 195 K. The complete data are compiled in Table 3.

Also contained in Fig. 9 is the H_2 adsorption isotherm at 77 K for a molybdena–alumina catalyst ($e/Mo = 1.7$) poisoned

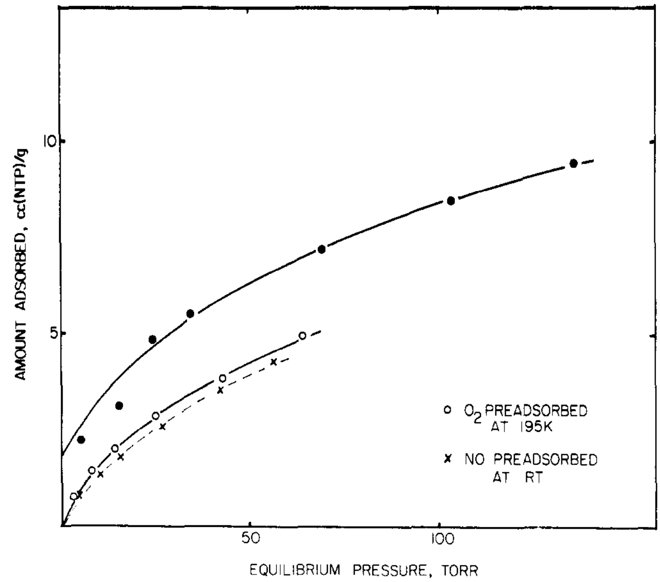

FIG. 9. The hydrogen adsorption isotherm at 77 K for 8% Mo/Al_2O_3 reduced to *e*/Mo = 1.7 (●); with 1.5 cm^3(NTP)/g O_2 poisoning (O); with 5.0 cm^3(NTP)/g NO poisoning (X).

with NO; this gas (which is not as selective as O_2) was preadsorbed [5.0 cm^3(NTP)/g] and evacuated at room temperature prior to the low-temperature hydrogen adsorption. The isotherm fell almost exactly on that obtained in the oxygen poisoning studies and the observed linewidth, although slightly greater at low coverages than that observed for O_2 poisoning, was still far below the linewidth from the unpoisoned adsorption. The data are included in Table 3 and plotted in Fig. 10.

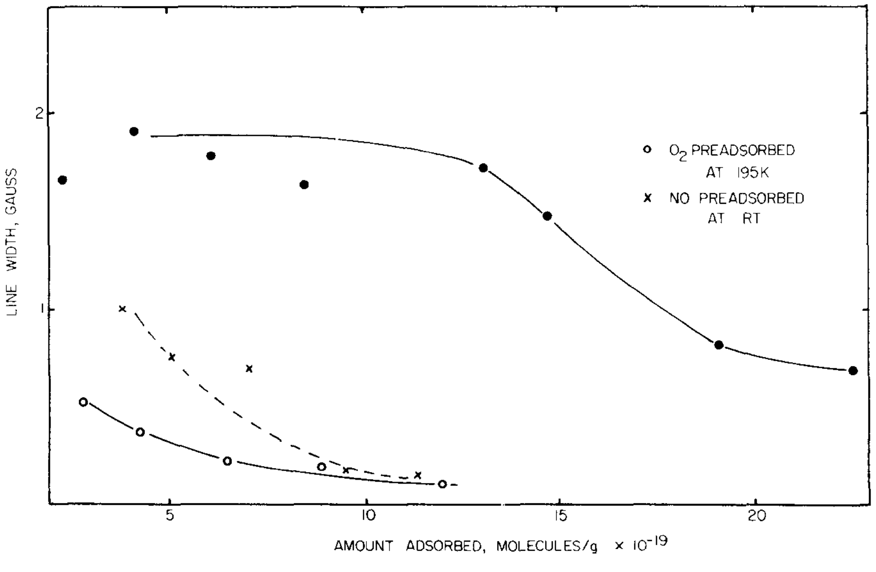

FIG. 10. A plot of the observed linewidth at 35 MHz versus the amount adsorbed for H_2 adsorption at 77 K on 8% Mo/Al_2O_3 reduced to *e*/Mo = 1.7 (●); with 1.5 cm^3(NTP)/g O_2 poisoning (O); with 5.0 cm^3(NTP)/g NO poisoning (X); the line for an unreduced catalyst approximates that through the open circles, see Fig. 7.

TABLE 3

A Summary of Volumetric and NMR Data for H_2 Adsorption at 77 K on Reduced Molybdena–Alumina (e/Mo = 1.7) Poisoned with Either O_2[a] or Nitric Oxide[b]

Sample	Equilibrium pressure (Torr)	Adsorbed volume (cm^3 (NTP)/g)	Linewidth[c] (G)
Molybdena–alumina (e/Mo = 1.7)	0.75	1.52	1.9
	5.30	2.23	1.8
	15.50	3.16	1.63
	24.20	4.90	1.72
	34.35	5.51	1.47
	69.25	7.16	0.91
	102.75	8.45	0.68
	135.15	9.37	0.54
O_2 poisoning at 195 K	3.20	0.83	—
	8.55	1.48	0.63
	14.30	2.05	0.48
	25.35	2.87	0.33
	42.90	3.82	0.32
	63.30	4.97	0.21
Nitric oxide poisoning at room temperature	5.80	0.90	—
	10.75	1.42	1.0
	15.35	1.86	0.8
	26.70	2.65	0.73
	41.80	3.57	0.28
	56.20	4.30	0.27

[a] 1.5 cm^3(NTP)/g of O_2 was irreversibly adsorbed at 195 K.

[b] 5.0 cm^3(NTP)/g of NO was irreversibly adsorbed at room temperature.

[c] Corrected for finite modulation amplitude (*14*).

DISCUSSION

The adsorption of hydrogen on alumina and molybdena–alumina at 77 K is rapid and reversible and has most of the attributes expected of physical adsorption. However, measurements of the separation factors for H_2 from D_2 (*8*) have suggested molecular chemisorption with a substantial barrier to rotation on sites having a strong electric field gradient. Moreover, the adsorption occurs far below monolayer coverage and obeys the Freundlich law (*10*). A stronger underlying type of chemisorption is indicated by the dependence of the linewidth of the NMR data upon coverage.

The hydrogen adsorption isotherms at 77 K for both γ-alumina and molybdena–alumina were fitted accurately by the Freundlich equation (*10*)

$$\theta = kp^{1/n}, \qquad n > 1, \tag{2}$$

where $\theta = V_{\mathrm{ads}}/V_{\mathrm{m}}$, $n = Q_0/RT$, and Q_0 is a parameter which indexes the distribution of heats. The Freundlich treatment includes the assumption of an exponential distribution of site energies, with each type of site having a characteristic heat of adsorption. Equation (2) may be cast into a more useful form by including the V_{m} term in the constant and taking the logarithm of both sides

$$\ln V_{\mathrm{ads}} = \ln k' + 1/n \ln p. \tag{3}$$

Plots of $\ln V_{\mathrm{ads}}$ versus $\ln p$ for the molybdena–alumina catalysts gave straight lines with slopes of $1/n$ for all catalysts studied. The Freundlich parameters derived are listed in Table 4. These values increased substantially as the molybdena–alumina was reduced. As shown in Fig. 11, n was an index for important catalytic properties determined in other work. Plots of irreversibly chemisorbed hydrogen (*10*) and/or the rate constant for propylene hydrogenation (*16*) versus n gave straight lines suggesting that the ability of the catalyst to activate hydrogen and hence to hydrogenate olefins is "turned on" as the catalyst is reduced. Even though these properties may stem from the creation of a relatively small number of special sites, it is evident that the whole distribution is altered.

Millman and Hall (*10b*) suggested that the same sites which chemisorb hydrogen irreversibly at 77 K may also be responsible for the room-temperature catalytic reaction. Our data show that the activity of the surface for both these processes is related to the distribution of the adsorption potential, indexed by the parameter, n. In a related study, Millman *et al.* (*10a*) showed that on molybdena–alumina catalysts, the strength of the surface field gradient is reflected by the separation factor (S) for H_2 and D_2 adsorption at 77 K. It was reported that S increased with extent of reduction for e/Mo < 1; above this value, S leveled off. The authors explained this phenomenon by suggesting that dissociation of the adsorbed molecules became important around this

TABLE 4

Comparison of the Freundlich Parameters Determined by the Volumetric and NMR Methods for H$_2$ Adsorbed on Alumina and Molybdena–Alumina Catalysts

Sample	Pretreatment temp (°C)	Adsorption temp (°K)	Parameter, n		(k')[a]
			Volumetric	NMR	
γ-Alumina					
M.K. R&D	550	80	1.36	1.35	0.167
	550	100	1.27	1.5	0.057
	550	120	1.18	1.1	0.016
CK-300	500	77	1.19	1.2	0.106
Molybdena–alumina					
e/Mo = 0	500	77	1.34	1.6	0.192
e/Mo = 0.25	500	77	1.51	0.7	0.259
e/Mo = 0.8	500	77	1.53	0.4	0.423
e/Mo = 1.1	500	77	1.48	0.3	0.353
e/Mo = 1.3	500	77	1.85	—	—
e/Mo = 1.7	500	77	2.69	—	1.43

[a] From Eq. (3).

value; this was reflected by the observation of rapid H$_2$–D$_2$ exchange. Thus, at the point where dissociation became appreciable, a maximum in S developed accompanied by a sharp increase in n, H_{irr}, and the rate of propylene hydrogenation; significant changes also occurred in the NMR data presented below.

Kazansky and co-workers (*11*) proposed the use of NMR for the study of gas–surface interactions in cases where rapid exchange occurs between physisorbed and chemisorbed molecules. In general, the NMR linewidth of a chemisorbed molecule will be broader than that of a physisorbed molecule. If a rapid exchange exists between the two types of species, an averaged resonance line will be observed, whose

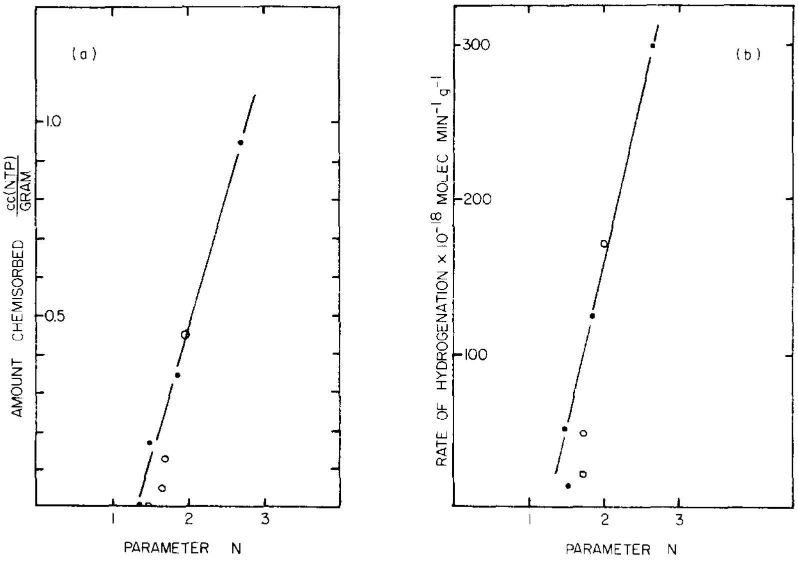

FIG. 11. Plots of (a) H_{irr} at 77 K from Ref. (*10*) or (b) the rate of propylene hydrogenation from Ref. (*16*) versus the Freundlich parameter, n.

linewidth and position may be described by the equations

$$\Delta H = \chi_c \Delta H_c + \chi_{ph} \Delta H_{ph}, \quad (4)$$

$$\delta = \chi_c \delta_c + \chi_{ph} \delta_{ph}, \quad (5)$$

where χ_c and χ_{ph} are mole fractions; δ_c and δ_{ph} are chemical shifts; and ΔH_c and ΔH_{ph} are linewidths for the chemisorbed and physisorbed molecules, respectively. Since $\chi_c + \chi_{ph} = 1$ and $\chi_c = c/V$, where c is the constant amount of chemisorbed species and V is the total amount adsorbed ($V \gg c$), we may write

$$\chi_{ph} = 1 - c/V. \quad (6)$$

Substitution of (6) into (4) yields

$$\Delta H = \Delta H_{ph} + c/V\,(\Delta H_c - \Delta H_{ph}). \quad (7)$$

Thus, the term ΔH_{ph} may be obtained either graphically from the intercept of a plot of linewidth versus V_{ads}^{-1}, or experimentally from the limiting value of the linewidth at high coverage; H_c may be obtained from the slope of the above-mentioned plots. Implied in this treatment is the assumption that all the chemisorption sites are filled at all coverages. This behavior was exhibited by both the alumina samples and the unreduced catalysts. Linewidths for the chemisorbed hydrogen (ΔH_c) were calculated as 32.5 and 15.6 G, respectively.

Kibby *et al.* (*12*) used Eq. (7) with the Langmuir isotherm to derive an expression relating the NMR line broadening to the equilibrium pressure of the adsorbate. In this manner, they were able to calculate equilibrium constants and heats of adsorption for ethylene adsorbed on silica–alumina and for Co^{2+} or Ni^{2+} on silica catalysts. Our data for the low-temperature adsorption of H_2 on alumina and molybdena–alumina could not be fitted by a Langmuir isotherm, but were accurately described as Freundlich (see previously). The theory was therefore modified such that

$$(\Delta H - \Delta H_{ph}) = c/k'\,(\Delta H_c - \Delta H_{ph}) p^{1/n}. \quad (8)$$

If the above-mentioned conditions exist, viz., Freundlich behavior for the total adsorption and rapid exchange between chemisorbed and physisorbed species, a plot of ln ($\Delta H - \Delta H_{ph}$) versus ln p should give a straight line of slope $-1/n$. Both the alumina support and the unreduced molybdena–alumina catalysts produced NMR data which could be described by Eqs. (7) and (8). Values of n so calculated were found to be in reasonable agreement with those obtained from the volumetric data (Table 4). The results taken from the reduced catalysts, however, were not; they have been included to illustrate the failure of the theory to describe the experimental NMR data for these samples. This is not a failure of the Freundlich equation to describe the adsorption data, but of Eq. (7) to describe the exchange processes. As shown in Fig. 12, two slopes were obtained for the reduced samples. These indicate an abrupt change in the adsorption process at the break points. Presently, we are unable to interpret these observations, except to note that new complicating features have been introduced by the reduction. For example, the increase in the value of coverage at the break points follows the increase in the extent of reduction and this behavior mimics that of the vacancy concentration (*13*). Moreover, an increasing portion of the adsorbed hydrogen becomes dissociated and this ultimately leads to the plateau(s) appearing in Fig. 6. Millman and Hall (*17*) have demonstrated the importance of multiple coordinative unsaturation in the irreversible adsorption of hydrogen on reduced molybdena–alumina at 77 K. Following this type of argument, the initial adsorption of H_2 on the multiply coordinatively unsaturated sites might differ from subsequent adsorption on the partially occupied sites, and thus could be responsible for the breaks in the data in Fig. 12. The chemisorption of poison molecules substantially reduced the amount of hydrogen adsorbed (Fig. 9). This decrease was comparable with the amount of poison used and

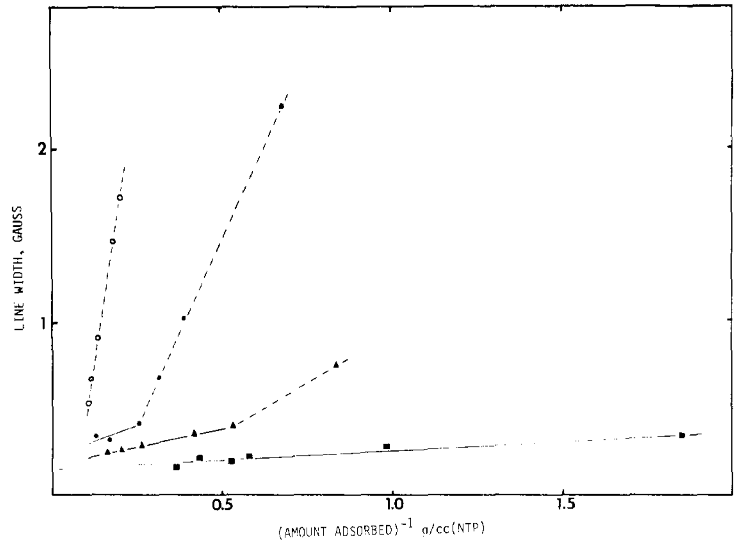

FIG. 12. A plot of the observed linewidth (35 MHz) versus the reciprocal of the amount adsorbed for H_2 adsorption at 77 K on molybdena–alumina: unreduced (■); reduced to e/Mo = 0.25 (▲), 1.1 (●), and 1.7 (○).

within a factor of 2 or 3 of the values of the adsorption at the high ends of the plateau (Fig. 7). Whereas these do not match the values of the adsorption at the break points, they again are not greatly different. This same poison converted the linewidth dependence on coverage from that of a reduced catalyst to that of an unreduced one, although the amount added was not sufficient to change the oxidation state materially.

Data for the alumina catalysts were in general agreement with the theory (*11, 12*). If the relationship between vacancy concentration and low-temperature chemisorption of hydrogen exists as suggested previously (*7*), the amount adsorbed should increase with increasing pretreatment temperature; this was observed in Fig. 1. However, the corresponding increase in the observed linewidth, shown in Fig. 2, could be due to either an increase in the number of chemisorption sites or to an increase in the average site strength, or both, since these features are related.

The strong dependence of T_1 on surface coverage, shown in Fig. 3, suggests that the interaction with the surface provides the mechanism for relaxation. Intermolecular processes, viz., collisions between adsorbate molecules, may be dismissed on the basis of the deuterium substitution data shown in Fig. 4. Intramolecular processes may account for a portion of T_1, but an increase in the average site strength should lead to a larger value of T_1 as the coverage is lowered (a larger fraction of the molecules would be strongly held by the surface, thus weakening the interaction between the ^1H nuclei in the pairs). In fact, the opposite was observed (Fig. 3). Therefore, if this pathway is present, it contributes only a small portion of the total. Thus, it seems that the proton spin–lattice relaxation results from interactions with the surface; however, the available evidence is insufficient to distinguish among the possible mechanisms, viz., relaxation due to proton translational diffusion, relaxation due to spin–energy diffusion to paramagnetic centers (impurities), or relaxation through neighboring ^{27}Al cations. Because of the high purity of the alumina used (*8*), the effect of paramagnetic centers probably can be dismissed. Figure 3 contains evidence for relaxation due to both proton translational diffusion and interaction with ^{27}Al (CUS). For increasing temperatures at constant coverage, T_1 decreased for each preparation as required for relaxation by translational diffusion. At the same time, for constant adsorption temperature and constant coverage, T_1 decreased with the extent of dehydroxylation, as expected for interaction with ^{27}Al (CUS). This latter effect is of direct interest to the understanding of the nature of the chemisorption phenomenon.

Attempts to measure the longitudinal relaxation time (T_1) of hydrogen adsorbed on molybdena–alumina catalysts were unsuccessful, since the observed resonance would not saturate. This result is interesting because it suggests the importance of paramagnetic centers in the relaxation process. Pulse NMR studies of this system should be performed to determine the nature of this interaction.

Effects of Reduction

The appearance of the plateau(s) in Fig. 7 for catalysts reduced beyond $e/Mo \sim 1.1$ leads to a paradox. The value of the linewidth corresponds to that observed previously (*18*) for the surface hydroxyl groups on these catalysts. Strong magnetic interactions with either Al^{3+} (CUS) or paramagnetic centers (e.g., Mo^{5+}, Mo^{4+}, or Mo^{3+}) will remove a substantial portion of these (up to 80% for an extensively reduced catalyst) from detection by NMR (*18*). Thus, the weak resonance lines corresponding to the plateau region at low H_2 coverages should represent only a portion of the adsorbed hydrogen. Measurements of integrated intensities, although not very precise in this region, did show that only a fraction of the adsorbed hydrogen was being observed. Moreover, the plateau appears at the same extent of reduction for which the rate of H_2–D_2 exchange became easily measurable (*10*), strengthening the suggestion of dissociative adsorption. Reductive adsorption seems unlikely, since the formation of some low-valence molybdenum species (e.g., Mo^{4+} or Mo^{3+}) near the adsorbed hydrogen would probably prevent detection of the ^1H by NMR. Oxidative adsorption would require a relatively large concentration of lower-valence molybdenum species (*4*); this is believed not to be the case. Heterolytic dissociative adsorption seems the most acceptable alternative. However, if the hydroxyl groups detected by NMR occur on the alumina surface (see previously), how is their formation influenced by the molybdena layer? Recent infrared and NMR data (*15, 18*) suggested that the reduction process at 500°C may lead to attack of hydrogen at the interface of the molybdena and alumina layers. Moreover, the reversibly held hydrogen (H_R) was shown to be heterolytically cleaved upon adsorption. If the reduction process corresponds to a "peeling back" of the molybdena adlayer, the sites exposed on the alumina surface are likely candidates for H_2 molecular chemisorption. This is supported by the data in Fig. 8 which show that the dehydroxylated alumina surface is "healed" by the addition of the molybdena layer. Only after reduction does the averaged linewidth become equal to that of the original alumina. Furthermore, as the extent of reduction increases, there is evidence for dissociative adsorption, perhaps due to an increase in the number of sites that are multiply coordinatively unsaturated. The poisoning data obtained with O_2 and/or NO support this hypothesis. However, the problem of the nature of some of the sites remains, since the NMR experiment observes only those species which are remote from paramagnetic centers.

ACKNOWLEDGMENT

The authors gratefully acknowledge the support of the National Science Foundation (Grant CHE77-07772) for this research. Our thanks are also due to the Laboratory for Surface Studies at the University of Wisconsin–Milwaukee for partial salary support.

REFERENCES

1. Trapnell, B. M. W., *in* "Catalysis" (P. H. Emmett, Ed.), Vol. III, p. 1. Reinhold, New York, 1955.

2. Eley, D. D., *in* "Catalysis" (P. H. Emmett, Ed.), Vol. III, p. 60. Reinhold, New York, 1955.
3. Eischens, R. P., Pliskin, W. A., and Low, M. J. D., *J. Catal.* **1**, 180 (1962).
4. Burwell, R. L., Jr., and Stec, K., *J. Colloid. Interface Sci.* **55**, 54 (1977).
5. (*a*) Kokes, R. J., *Acc. Chem. Res.* **6**, 226 (1973); (*b*) Dent, A. L., and Kokes, R. J., *J. Phys. Chem.* **73**, 3772 (1969).
6. Burwell, R. L., Jr., Haller, G. L., Taylor, K. C., and Read, J. R., *in* "Advances in Catalysis" (D. D. Eley, H. Pines, and P. B. Weisz, Eds.), Vol. 20, p. 1. Academic Press, New York, 1969.
7. Hall, W. K., *Acc. Chem. Res.* **8**, 257 (1975).
8. Van Cauwelaert, F. H., and Hall, W. K., *J. Colloid Interface Sci.* **38**, 1 (1972); *Trans. Faraday Soc.* **66**, 454 (1970).
9. Chang, C. C., and Kokes, R. J., *J. Amer. Chem. Soc.* **93**, 7107 (1971).
10. (*a*) Millman, W. S., Van Cauwelaert, F. H., and Hall, W. K., *J. Phys. Chem.* **83**, 2764 (1979); (*b*) Millman, W. S., and Hall, W. K., Preprint of paper submitted for VIIth International Congress on Catalysis, Tokyo, July (1980).
11. Kazansky, V. B., *Proc. VIth Int. Congr. Catal.* **1**, 50 (1976).
12. Kibby, C. L., Borovkov, V. Yu., Kazansky, V. B., and Hall, W. K., *J. Catal.* **46**, 275 (1977).
13. Lo Jacono, M., and Hall, W. K., *Proc. VIth Int. Congr. Catal.* **1**, 246 (1976).
14. Smith, G. W., *J. Appl. Phys.* **35**, 1217 (1964).
15. Millman, W. S., Crespin, M., Cirillo, A. C., Jr., Abdo, S., and Hall, W. K., *J. Catal.*
16. Lombardo, E. A., and Hall, W. K., to be published.
17. (*a*) Millman, W. S., and Hall, W. K., *J. Phys. Chem.* **83**, 427 (1979); (*b*) *J. Catal.* **59**, 311 (1979).
18. Cirillo, A. C., Jr., Dollish, F. R., and Hall, W. K., *J. Catal.*, in press; Paper presented at VIth N.A. Meeting of Catalysis Society Chicago, March 1979.